Published in final edited form as:
Clin Cancer Res. 2014 September 1; 20(17): 4673–4688. doi:10.1158/1078-0432.CCR-14-0363.

To "Grow" or "Go": TMEM16A Expression as a Switch between Tumor Growth and Metastasis in SCCHN

Daniel J. Shiwarski[1,2,*], **Chunbo Shao**[7], **Anke Bill**[8], **Jean Kim**[1], **Xiao Dong**[1], **Carol A. Bertrand**[3], **Raja S. Seethala**[4], **Daisuke Sano**[5], **Jeffery N. Myers**[6], **Patrick Ha**[7], **Jennifer Grandis**[1], **L. Alex Gaither**[8], **Manojkumar A. Puthenveedu**[2], and **Umamaheswar Duvvuri**[1]

[1]VA Pittsburgh Health System & Department of Otolaryngology, University of Pittsburgh Medical Center, Pittsburgh, PA, USA

[2]Department of Biological Sciences, Carnegie Mellon University, Pittsburgh PA

[3]Cell Biology, University of Pittsburgh Medical Center, Pittsburgh, PA, USA

[4]Pathology, University of Pittsburgh Medical Center, Pittsburgh, PA, USA

[5]Yokohama City University, School of medicine, Yokohama, Japan

[6]Department of Head and Neck Surgery, The University of Texas MD Anderson Cancer Center, Houston, Texas, USA

[7]Department of Otolaryngology Johns Hopkins University School of Medicine, Baltimore, MD, USA

[8]Department of Developmental and Molecular Pathways, Novartis Institute for Biomedical Research Inc.

Abstract

Purpose—Tumor metastasis is the leading cause of death in cancer patients. However, the mechanisms that underlie metastatic progression remain unclear. We examined TMEM16A (ANO1) expression as a key factor shifting tumors between growth and metastasis.

Experimental Design—We evaluated 26 pairs of primary and metastatic lymph node tissue from patients with squamous cell carcinoma of the head and neck (SCCHN) for differential expression of TMEM16A. Additionally, we identified mechanisms by which TMEM16A expression influences tumor cell motility via proteomic screens of cell lines and *in vivo* mouse studies of metastasis.

Results—Compared to primary tumors, TMEM16A expression decreases in metastatic lymph nodes of patients with SCCHN. Stable reduction of TMEM16A expression enhances cell motility and increases metastases while decreasing tumor proliferation in an orthotopic mouse model. Evaluation of human tumor tissues suggests an epigenetic mechanism for decreasing TMEM16A

Address Correspondence to: Umamaheswar Duvvuri MD, PhD, 200 Lothrop Street, W948 Biomedical Science Tower, University of Pittsburgh Medical Center, Pittsburgh, PA 15213, (412)-647-0954 (Tel), (412)-383-5407 (Fax), duvvuriu@upmc.edu.
*Present address: Department of Biological Sciences, Carnegie Mellon University, Pittsburgh PA.

The contents do not represent the views of the Department of Veterans Affairs, or the United States Government. L Alex Gaither and Anke Bill are employees of Novartis Institutes for Biomedical Research

expression through promoter methylation that correlated with a transition between an epithelial and a mesenchymal phenotype. These effects of TMEM16A expression on tumor cell size and epithelial to mesenchymal transition (EMT) required the amino acid residue, serine 970 (S970); however, mutation of S970 to alanine does not disrupt the proliferative advantages of TMEM16A overexpression. Further, S970 mediates the association of TMEM16A with Radixin, an actin-scaffolding protein implicated in EMT.

Conclusions—Together, our results identify TMEM16A, an eight trans-membrane domain Ca^{2+}-activated Cl^- channel, as a primary driver of the "Grow" or "Go" model for cancer progression, in which TMEM16A expression acts to balance tumor proliferation and metastasis via its promoter methylation.

Keywords

Head and neck/oral cancers; Cell adhesion; Cell signaling; Cell motility and migration; Metastasis/metastasis genes/metastasis models; Tumor markers and detection of metastasis; DNA methylation/epigenetics; Protein/protein interactions

Introduction

One of the main predictors of survival for patients with squamous cell carcinoma of the head and neck (SCCHN) is the presence of nodal metastases; however, little is understood about the mechanisms that underlie its development (1). Patients with SCCHN often suffer from locally advanced disease and inevitable recurrence despite aggressive treatments. Any additional insight into the driving force behind tumor progression towards metastasis would be translationally and scientifically beneficial for all patients with advanced disease.

Generally, tumor progression requires both tumor growth and subsequent metastatic development. The cellular events driving this progression require complex coordinated regulation of both growth and motility pathways. These complementary pathways exist in a balance, whereby tumor cells can oscillate between states through precise molecular alterations. Gil-Hen et al. have reported that tumor cells have the ability to manipulate intracellular signaling pathways to independently induce tumor growth while diminishing metastasis (2).

Here, we implicate TMEM16A as a critical factor that can independently shift tumors between the growth and metastatic states. TMEM16A is an eight trans-membrane domain Ca^{2+}-activated chloride channel (3). It is localized to the 11q13 chromosomal amplicon, and is frequently overexpressed in many solid malignancies including breast cancer, bladder cancer, and SCCHN (4,5). We have recently reported that when TMEM16A is overexpressed in primary SCCHN it directly contributes to tumor proliferation via activation of the RAS-RAF-ERK-CCND1 pathway and correlates with decreased patient survival (6). The role of TMEM16A expression in an *in vivo* metastasis setting has not been tested. Additionally, the molecular mechanisms underlying potential contributions of TMEM16A expression on cell motility and metastasis remain unknown. Our goal was to conclusively determine the direct effects of stable TMEM16A expression on tumor progression towards metastasis *in vivo*.

Specifically, our results indicate that increasing TMEM16A expression promotes primary tumor growth and decreases motility, while decreased expression slows proliferation allowing for metastatic progression. We show that TMEM16A expression is downregulated in metastatic lymph nodes when compared to paired primary SCCHN tumors from human patients. Using both *in vitro* and *in vivo* systems, we demonstrate that TMEM16A, through its S970 amino acid, directly influences tumor cell motility and metastases by impacting epithelial-to-mesenchymal transition and expression of cytoskeletal and adhesion molecules, independently of its growth characteristics. Further, S970 is required for the interaction between TMEM16A and the actin-scaffolding protein Radixin. In addition, *in vivo* expression of TMEM16A is controlled by promoter methylation, a novel mechanism by which *TMEM16A* gene expression is regulated. These data identify *TMEM16A* promoter hypermethylation as a key driving factor for the transition of tumor cells between proliferative and metastatic states, a central idea in the transformative “Grow and Go” model for tumor progression.

Materials and Methods

Cell culture

All cell lines were used after genotype verification. UM-SCC1 and T24 cells were obtained from the University of Michigan (a gift of Dr. Tom Carey). HN5 and FaDu cells were obtained from ATCC. Stable overexpressing clones were made using DNA transfection or retroviral infection. All cell lines were grown in DMEM with 10% Fetal Bovine serum.

Immunoblotting

For immunoblotting, equal amounts of protein were separated on SDS-PAGE, and transferred to nitrocellulose membranes. The membranes were then probed with the appropriate antibodies. A complete list of antibodies is provided in Supplemental Table 3.

Immunoprecipitation protocol

HEK-293T cells were transfected with the indicated plasmids. Cell lysates were prepared 48 hours post-transfection. TMEM16A was immunoprecipitated using the SP31-clone with agarose beads. Immunocomplexes were subsequently resolved using SDS-PAGE and probed using the corresponding antibodies.

Plasmid/siRNA transfections, retrovirus generation, shRNA transduction

Plasmid transfections were performed using either Fugene (DNA) or Lipofectamine2000 (siRNA) according to the manufacturer’s instructions. TMEM16A cDNA was subcloned into pBabe-puro vector. Retroviruses were generated by transfecting HEK-293T PhoenixAmpho cells and collecting virus containing media 48–72 hours post transfection. Lentiviral shRNA and retroviral particles were used to transduce cells with polybrene or sequbrene. Appropriate antibiotic selection was performed 72–96 hours after viral transduction.

Transwell Migration Assay

Transwell inserts (BD Biocoat™, 8.0 micron) were used to assess the amount of cells that migrated through the chamber from serum-free media on the inside towards a serum containing media on the outside. Cells were fixed and stained 24 hours after plating using HEMA 3 solutions (Protocol). Multiple independent fields were arbitrarily chosen and counted for each replicate. For invasion assays, we conducted the same protocol as for the migration assay using BD BioCoat™ Growth Factor Reduced BD Matrigel™ Invasion Chamber, 8.0 μm PET Membrane 24-well Cell culture inserts.

Wound Healing Assay

The cells were plated in DMEM plus 10% Fetal Bovine Serum in a 6-well culture plate and grown to confluence. Once confluent, a wound was inflicted and images were captured at 0 hours and 24 hours post wound. To assess the amount of movement during wound closure, we calculated the area of the initial wound and subtracted from that the final area of the wound 24 hours later using Image J software. This calculation of the difference between the initial and final areas allowed for a consistent measurement of movement regardless of inconsistencies in the wound itself.

E-cadherin Luciferase Assay

E-cadherin promoter activity assay was performed as previously reported (7). An E-cadherin luciferase reporter construct and Renilla control plasmid were transfected using Lipofectamine 2000 into T24 cancer cells. The luciferase activity was evaluated 24 hours after the transfection using the Promega Dual Luciferase kit. The samples were read using a luminometer according to the Promega protocol, and the amount of individual florescence was normalized to the amount of Renilla luciferase and total protein concentration for each sample.

Densitometry

Densitometry from digital scans of X-ray film after immunoblotting was performed using Image J software and quantification via the LiCor Odyssey Imaging system when applicable.

Primary tissue samples

Paired primary and metastatic tissues were collected after obtaining informed consent and approval from the University of Pittsburgh Institutional Review Board. Tissue samples were formalin fixed and paraffin embedded from patients who underwent curative surgery for SCCHN at our institution. Staining was performed with anti-TMEM16A antisera (clone SP31 ThermoFisher). Slides were scored using a semi-quantitative system.

Cell Size Measurements

T24 cancer cells were plated onto 35mm MatTek dishes at 50% confluence. The cells were imaged with a 40x objective and borders were drawn to measure the cell size as total area. Area was measured in microns^2. Additionally, FACS was performed by plotting forward

scatter compared to side scatter to establish a comparative cell size for the T24 control, TMEM16A overexpression, scrambled shRNA control, and TMEM16A shRNA cell lines.

Bisulfite treatment and Quantitative methylation-specific PCR

The EpiTect Bisulfite Kit (Qiagen) was used to convert unmethylated cytosines in DNA to uracil according to the manufacturer's instructions. Quantitative methylation-specific PCR (qMSP) was carried out in a 7900 sequence detector (Perkin-Elmer Applied Biosystems, Carlsbad, CA) and analyzed by a sequence detector system (SDS 2.3; Applied Biosystems), as previously described (8). The *TMEM16A* qMSP primer sequences designed were: Forward 5′- AGGATCGTAGCGTTTATATTA −3′, and Reverse 5′- CGCGACCCTCCCGCC −3′. The *TMEM16A* qMSP probe sequence was 6FAM 5′- CGCACTCACCGTACCCTCG −3′ TAMRA. The primers and probe sequences for β-actin (an internal reference standard) and detailed qMSP PCR conditions are described by Shao, et al (8).

Leukocyte DNA from a healthy individual was methylated *in vitro* with excess *Sss*I methyltransferase (New England Biolabs, Inc., Ipswich, MA) to generate completely methylated DNA. Serial dilutions (30–0.003 ng) of this bisulfite-treated methylated DNA were used to construct a calibration curve. All data points were within the range of sensitivity and reproducibility of the assay based on the calibration curve. The methylation levels in each sample were determined as a ratio of qMSP-amplified gene to β-actin (reference gene) and then multiplied by 1000 for easier tabulation (average value of gene triplicates divided by the average value of β-actin triplicates × 1000).

Mouse Xenografts

Implantation of tumor cells into the lateral tongues of nude mice generated orthotropic tumor xenografts. When tumors reached a critical size (or after 2 weeks), mice were sacrificed and tissues were harvested for histology. Lymph node metastases were determined by H&E staining of cervical lymph nodes.

Global Proteomic Analysis

T24 cells were stably transduced with viral constructs encoding scrambled control or TMEM16A shRNA lentiviral particles. Stabled pooled clones overexpressing TMEM16A or control plasmids were also generated. Cell pellets were harvested and lysed. Mass spectrometry methods were used to evaluate global expression changes(9,10). These data were then used to generate global protein expression changes in an unbiased fashion. Proteins that changed in a predictable fashion with TMEM16A manipulation (i.e, increased with TMEM16A overexpression AND subsequently decreased with TMEM16A knock down, or vice versa), were identified. This subset of proteins was then subjected to INGENTUITY analysis to identify cellular pathways that were affected with TMEM16A manipulation.

Cell viability assay

For proliferation and viability analysis, cells were plated in black walled 96-well optical plates at 5×10^3 cells/well. The CellTiter-Glo Assay (Promega) was used according to the

manufacturer's directions to establish proliferation viability for multiple cell lines and experimental conditions.

Quantitative Reverse Transcription (RT)-PCR

Taqman primers and probes were designed with the PRIMER EXPRESS V.2.0.0 program (Applied Biosystems, Foster City, CA). Reverse transcription was carried out as described (4,6,25). Quantitative Reverse Transcription PCR (qRT-PCR) was performed for *TMEM16A*, and *GAPDH* (used as an endogenous control). For E-cadherin and Snail mRNA evaluation, the primers and PCR conditions were chosen from Rosivatz et al. (11). All probes and primer were purchased from IDT DNA technologies as probe and primer mixes.

Statistical Analysis

Statistical analysis was performed using GraphPad Prism 4 or Stat Exact software. All data are reported as mean ± SEM unless stated otherwise. A paired t-test was used to evaluate differences in TMEM16A expression between paired primary and metastatic tumor tissue.

All experiments performed in mice were conducted after obtaining informed consent and approval from the University of Pittsburgh Institutional Animal Care and Use Committee. All human tissues were acquired after obtaining informed consent under Institutional Review Board approval.

Results

TMEM16A Expression is Decreased in Metastatic Nodal Tissue

We previously demonstrated that TMEM16A expression is increased in primary SCCHN tumors (6). Recent reports have suggested that TMEM16A overexpression might play a role in tumor cell motility (12). We therefore sought to determine if TMEM16A expression in patients with SCCHN varies between metastatic lymph node compared to paired primary tumors. We evaluated TMEM16A expression via immunohistochemistry in 21 SCCHN primary tumor/metastatic lymph node pairs. TMEM16A primary tumor expression was higher compared to paired metastatic tissue for 18 of 21 patients; in the remaining 3 patients, the expression was comparable. A representative example of three paired primary and metastatic nodal tissue samples is shown in Figure 1A. A semi-quantitative scoring of the IHC staining demonstrated a ∼50% decrease in TMEM16A expression levels in the metastatic tissue normalized to paired primary tissue (Figure 1B). Interestingly, TMEM16A expression in the primary tumor did not correlate with the development of nodal metastases (Supplementary Figure 1).

To determine if differences in TMEM16A expression between the primary tumor and metastatic nodal tissue were due to changes within the tumor cells themselves or an effect contributed by the surrounding stromal tissue, we decided to use immortalized cell lines isolated from either primary or metastatic nodal tissue, and evaluate them for TMEM16A expression. RNA was isolated from SCCHN cell lines derived from syngeneic paired primary and lymph node metastatic tissue (UPCI-4A/B and UM-SCC10A/B), and analyzed for differences in TMEM16A mRNA levels. TMEM16A mRNA expression was

significantly decreased in metastases-derived cell lines compared to their paired-primary line (Figure 1C). To determine if expression of TMEM16A was actively down-regulated during the formation of nodal metastases, we implanted SCCHN cell lines known to have endogenous expression of TMEM16A and to form spontaneous metastasis, FaDu and HN5, into the tongue of nude mice. After sufficient tumor growth, the primary tumors and any nodal metastatic tissues found were harvested and evaluated for TMEM16A protein expression. In both FaDu and HN5 tumors, the nodal metastatic tissue exhibited decreased TMEM16A expression compared to the primary tumor site (Figure 1D). The changes in expression during metastatic formation in these ectopic models suggest that TMEM16A changes expression throughout tumor progression towards nodal metastasis. Primary tumors exhibit high expression of TMEM16A, while expression in nodal metastases is diminished. This suggests a mechanism in which tumor cells with high TMEM16A expression can dynamically down-regulate gene expression to facilitate the formation of nodal metastasis.

TMEM16A Down-regulation Promotes Cell Migration and Increases Nodal Metastases

Given our prior data (Figure 1A-D), we hypothesized that a reduction in TMEM16A promotes the ability of tumor cells to establish nodal metastases. A fundamental trait a tumor cell must acquire in order to successfully metastasize is the ability to increase cell motility and migration. We therefore evaluated TMEM16A's influence on these metastatic phenotypes using a wound closure assay, and trans-well migration chambers respectively. To evaluate these characteristics independent of TMEM16A expression on tumor cell proliferation, we constructed stable knockdowns of TMEM16A with lentiviral shRNA, and performed wound closure and migration assays within a time period less than the cell lines doubling rate. UM-SCC1 tumor cells, an SCCHN-derived cell line harboring the 11q13 amplification, were stably transduced with TMEM16A shRNA, and knockdown was confirmed via immunoblotting (Figure 2A). The stable TMEM16A knockdown led to a ∼60% increase in motility when compared to scrambled shRNA control cells as assessed by wound closure assays (Figure 2A, 2B). Additionally, trans-well migration assays performed with the same stable cell line revealed a 2-fold increase in migration for TMEM16A shRNA cells compared to control (Figure 2C). To next determine the effects of TMEM16A knockdown in non-amplified cells, we evaluated motility and migration in T24 cancer cells, which lack 11q13 amplification. Similarly, stable knockdown of T24 cancer cells with TMEM16A shRNA demonstrated an increase in both motility assessed by wound-closure and trans-well migration compared to scrambled shRNA control cells (Supplemental Figure 2). Together, these results show that stable reduction of TMEM16A expression increases tumor cell motility and migration *in vitro* independent of 11q13 amplification status.

To determine if TMEM16A knockdown was sufficient to promote nodal metastases in a previously established SCCHN orthotopic mouse model, we implanted UM-SCC1 cells with stable TMEM16A shRNA knockdown in the floor of mouths of nude mice (11). In agreement with our previous work, UM-SCC1 TMEM16A-shRNA tumors demonstrated a decreased end tumor weight consistent with their reported decreased proliferation ability (Figure 2D) (6). Despite their reduced size, UM-SCC1 TMEM16A-shRNA tumors formed three-fold more metastatic nodules when compared to scrambled shRNA-derived tumors (Figure 2E). These *in vitro* and *in vivo* results suggest that decreased expression of

TMEM16A is sufficient to promote metastatic capabilities of SCCHN cells independent of tumor proliferation.

TMEM16A Overexpression Decreases Cell Migration and Invasion

In UM-SCC1 and T24 cancer cells, knockdown of TMEM16A expression promoted metastatic capabilities through increased motility, migration, and nodal metastasis formation. To next determine the effects of TMEM16A overexpression on cancer cell motility and migration, we focused on T24 cancer cells because of their moderate basal TMEM16A expression, and lack of 11q13 amplification. Immunoblotting confirmed stable overexpression of TMEM16A in T24 cell line clones (Supplemental Figure 3A). In these cells, TMEM16A stable overexpression, which was previously shown to promote tumor proliferation(6), was associated with a significant reduction of migration (Supplemental Figure 3A, B). This decrease in the migratory capability of TMEM16A overexpressing cells was recapitulated in our trans-well migration assays (Supplemental Figure 3C). Similar data showing reduced motility was obtained with UM-SCC1 cells overexpressing TMEM16A (Supplemental Figure 3E, F, G).

To verify the specificity of TMEM16A overexpression and eliminate the possibilities of nonspecific effects from protein overexpression, the TMEM16A overexpressing cell line was transduced with TMEM16A lentiviral shRNA to revert the phenotype caused by the overexpression. In our previous manuscript, we demonstrated that when the overexpessing cell line was stably transduced with TMEM16A lentivral shRNA the increase in proliferation gained from the TMEM16A overexpression is eliminated (6). To now investigate migration and invasion, we used Matrigel™ containing trans-well chambers to evaluate cell invasion through a substrate. The reduction in invasive migration conferred by TMEM16A overexpression was abrogated following infection with shRNA targeting TMEM16A (Supplemental Figure 3D). These data support the conclusion that increasing TMEM16A confers a decrease in tumor cell motility, migration, and invasion opposite its pro-proliferative effects.

Overexpression of TMEM16A Promotes an Epithelial Morphology and Increased Cell Size

Our data (Supplemental Figure 3) show that TMEM16A overexpression reduces the metastatic characteristics of cancer cells. Therefore, we hypothesized that increasing TMEM16A expression altered cell morphology in a way that would structurally discourage motility and invasion. We again elected to use the T24 cancer cell line to assess the effects of TMEM16A expression on cell morphology. These cells exhibited pro-metastatic mesenchymal characteristics at baseline, and appeared to undergo a mesenchymal to epithelial transition (MET) (13,14) upon overexpression of TMEM16A. Stable overexpression of TMEM16A substantially changed the visible cell morphology, inducing an epithelial phenotype characterized by rounded colony growth that is often inversely correlated with metastasis. T24 cells expressing a stable shRNA knockdown of TMEM16A had a visible mesenchymal appearance similar to the control cells (Figure 3A).

Another characteristic of a transition from a metastatic competent mesenchymal cell to an epithelial cell is a change in cell size. Decreased cell size is known to correlate with a

mesenchymal cell morphology to facilitating migration, while increased cell size correlates with a transition to an epithelial cell morphology and a less motile phenotype (15). In our T24 stable overexpressing and knockdown cell lines we evaluated individual cell area in microns and cell volume as assessed by flow cytometry to quantitate any induced changes in cell size. TMEM16A overexpression resulted in a 68% increase in cell area compared to control, whereas, the TMEM16A shRNA knockdown cells demonstrated a 35% reduction in cell area compared to scrambled shRNA (Figure 3B). In these same T24 cell lines, TMEM16A overexpression led to a significant increase in cell volume as accessed by shifted forward scatter values, and the TMEM16A shRNA knockdown demonstrated a significant decrease in cell volume (Supplemental Figure 4A, 4B). Representative results from the flow cytometry experiments depict this shift in forward scatter for the overexpressing and knockdown cell lines. These data, taken together, illustrate the influence of TMEM16A expression on the regulation of cell size and morphology independent from its influence on cell proliferation, but also suggests a possible mechanism by which changes in cell morphology could either promote or inhibit cell movement and metastatic characteristics by physically altering the rigidity of the cells.

TMEM16A Expression Promotes an Epithelial Phenotype and Alters Transcriptional Regulation of E-cadherin

During tumor progression towards metastasis, it is known that cell morphology and the actin cytoskeleton are altered through changes in expression of the epithelial protein E-cadherin and the mesenchymal protein Vimentin (16,17). The classical epithelial to mesenchymal transition (EMT), is characterized by a decrease in E-cadherin and an increase in vimentin expression, and is a hallmark of metastatic progression (18). Our data demonstrates that increasing TMEM16A expression increases cell size, decreases motility, migration, and invasion, and can visibly induce an epithelial morphology *in vitro*. These observations, taken together, are indicative of epithelial cell morphology, and are predicted to coincide with an increase in E-cadherin and reduction of Vimentin expression.

To determine the impact of TMEM16A expression on the regulation of E-cadherin expression we first assessed E-cadherin promoter activity. Using T24 TMEM16A stable overexpression cell line, we observed a four-fold increase in E-cadherin promoter activity when compared to the vector control (Figure 3C, Top). Further, T24 TMEM16A shRNA stable knockdown cells exhibited an 85% decrease in E-cadherin promoter activity when compared to scrambled shRNA control (Figure 3C, Bottom).

To conclusively determine if the effects of TMEM16A on E-cadherin were specific to changes in TMEM16A expression, we performed a rescue experiment. In T24 cells stably expressing TMEM16A shRNA, we rescued stable knockdown with shRNA insensitive cDNA (TMEM16A*). Quantification of the rescue effect was evaluated via qRT-PCR for TMEM16A mRNA (Supplemental Figure 5A). We further confirmed that the inhibition of cell proliferation caused by the TMEM16A shRNA was reverted upon co-expression of the TMEM16A* cDNA (Supplemental Figure 5B). E-cadherin mRNA levels were quantified via qRT-PCR for T24 shRNA knockdown and subsequent rescue cell lines. The cells transduced with the shRNA lentivirus had a 40% reduction in E-cadherin mRNA, which was

rescued by expression of TMEM16A*cDNA (Figure 3D). To corroborate these changes in E-cadherin, the mRNA expression of the E-cadherin transcriptional repressor Snail was also evaluated via qRT-PCR for the same cell lines. Snail mRNA expression increased more than 2-fold upon TMEM16A knockdown, and returned to control levels when transfected with the TMEM16A*cDNA (Figure 3E). Taken together, these results suggest that altering TMEM16A expression is sufficient to modulate the transcriptional activity and expression of E-cadherin, thus stimulating epithelial cell characteristics.

To further assess a shift from a mesenchymal protein profile in native T24 cancer cells towards an epithelial protein profile immunoblotting was performed on several common prominent candidates for evaluating mesenchymal to epithelial transition. Upon TMEM16A overexpression, the protein expression of epithelial markers E-cadherin and ZO-1 increased, while the mesenchymal proteins Vimentin, Fibronectin, and alpha-Smooth Muscle Actin decreased (Figure 3F). This observed shift in the T24 cell line protein profile confirms a mesenchymal to epithelial transition upon TMEM16A overexpression, and suggests TMEM16A as a driver of tumor cell morphology.

Unbiased Proteomics Analysis Reveals a Broad Range of Motility and Morphology Associated Proteins Affected by Altered TMEM16A Expression

We have shown that modulating TMEM16A expression has a significant affect on the overall metastatic capabilities of UM-SCC1 and T24 tumor cells through regulation of EMT; however, the global impact of altering TMEM16A expression and its influence on proteins associated with cytoskeletal rearrangements necessary to allow EMT and metastasis to occur are unknown. To elucidate the possible molecular pathways underlying the connection between TMEM16A expression and tumor cell metastasis, we used a quantitative-unbiased mass spectroscopy method to determine the overall changes in protein expression profiles in T24 TMEM16A stable overexpression and knockdown cell lines. Positive hits were defined as differentially expressed proteins that were altered reciprocally for TMEM16A overexpression and knockdown cells in a consistent and reproducible manner. Using a bioinformatic approach, we noted that of the proteins identified to change most significantly with TMEM16A expression modulation, two prominent categorical distinctions were in the regulation of cellular motility and cytoskeletal regulation.

In total, 27 proteins associated with cell motility or morphology were identified to be differentially regulated between the T24 TMEM16A overexpression and shRNA knockdown cell lines. To highlight the differential expression pattern between the proteins identified, a heat map of the average peptide counts from the quantitative-unbiased mass spectroscopy runs was constructed for the TMEM16A overexpression (OE) and TMEM16A shRNA cells normalized to the vector control or scrambled shRNA control cell lines expression (Figure 4A). The $\log_2$ ratio peptide count between the overexpression and vector control or shRNA knockdown and scrambled shRNA control are represented as a range in color from red (high) to green (low) values. A table depicting the protein gene IDs and $\log_2$ ratios compared to controls can be found in Supplemental Table 1.

To construct an interaction map for the proteins identified in this analysis; we conducted an Ingenuity Pathway Analysis for the motility related protein expression data of the T24

TMEM16A overexpressing cells compared to their control cells (Figure 4B). Notably, several of the proteins influenced by TMEM16A manipulation were related to the actin cytoskeleton and are known to be involved in cell motility. In particular, Annexin A2, Filamin A, and Radixin were revealed as pathway nodes and are known to influence cell motility as well as epithelial to mesenchymal transition (19,20). TMEM16A has also been shown to associate with the Ezrin-Radixin-Moesin family of proteins, which could act as a link between our observed affects on cell motility and morphology by facilitating an interaction with the actin cytoskeleton (21). Therefore, we focused our further investigations on these candidate proteins.

To validate the data obtained from this global analysis, we choose Annexin A2, Filamin A, and Radixin to examine via immunoblotting. Immunoblotting results confirmed a decrease in Annexin A2 and Filamin A expression in T24 TMEM16A overexpressing cells, while Radixin expression was increased compared to control (Figure 4C). Densitometry was performed for each protein (n=3) to allow for a quantified comparison to the mass spectroscopy data (Figure 4D). These results suggest the possibility that TMEM16A can regulate EMT through interactions with the actin cytoskeleton to promote an epithelial phenotype.

TMEM16A S970 Interacts Directly with Radixin and is Required for TMEM16A's Effects on Cell Morphology and EMT

From our proteomic analysis, the actin associated protein Radixin appeared to be a good candidate for a mechanism by which TMEM16A could modulate the actin cytoskeleton stability to influence cell morphology and metastasis. Radixin, in cooperation with Ezrin and Moesin, is known to drive and stabilize the association between actin and the plasma membrane. Therefore, we hypothesized that TMEM16A's effects on cell morphology and EMT could be dependent upon a direct protein-protein interaction to Radixin that would sequester it away from its actin interactions. A comparative evaluation of the TMEM16A amino acid sequence to known Ezrin-Radixin-Moesin (ERM) binding sites revealed a possible ERM binding domain coordinated around Serine-970 within TMEM16A's cytoplasmic tail. To determine if TMEM16A S970 is required for TMEM16A's interaction with Radixin, we mutated the S970 to an alanine (S970A) and performed an immunoprecipitation between TMEM16A and HA-tagged Radixin in HEK-293T cells. Wild-type TMEM16A was found to directly interact with Radixin in HEK-293T cells via our immunoprecipitation experiment, exemplified by a prominent band of approximately 80kDa (Figure 5A). When performed with the mutated TMEM16A S970A construct, no apparent band for Radixin was observed after immunoprecipitating for TMEM16A and blotting for Radixin in HEK-293T cells (Figure 5A). This immunoprecipitation was repeated thrice and quantified via densitometry. A significant increase in the interaction between TMEM16A and Radixin was observed; however, upon mutation of the S970 to an alanine the association was lost (Figure 5B).

We next wanted to determine if the TMEM16A S970 residue is required for the effects contributed by TMEM16A expression on cell morphology and EMT. Stable expression of TMEM16A S970A in T24 cells was generated in pooled clones after transfection. The

expression of TMEM16A S970A did not induce an increase in the overall cell size normally associated with TMEM16A overexpression as assed by flow cytometry (Figure 5C). Additionally, overexpression of TMEM16A S970A did not promote an increase in the expression of E-cadherin and a decrease in the expression of Vimentin via immunoblotting (Figure 5D). To further confirm that expression of the TMEM16A S970A did not induce E-cadherin transcription, we evaluated the E-cadherin promoter activity and mRNA expression. Overexpression of TMEM16A S970A has no significant effect on increasing E-cadherin promoter activity or mRNA expression, as well as no effect on the transcriptional repressor for E-cadherin, Snail (Figure 5E, F, G). Finally, if TMEM16A S970 is required for to promote an epithelial phenotype, we next asked if the increased expression of TMEM16A S970A would promote an increase in tumor cell proliferation independent from its ability to influence EMT. We performed a cell proliferation assay using Cell Titer-Glo from Promega to determine the rate of cell proliferation after 3 days of growth in either normal adherent growth conditions or anchorage independent growth conditions using poly-Hema. In both anchorage independent and attached growth conditions stable overexpression of TMEM16A and TMEM16A S970A exhibited a 3–4 fold increase in proliferation (Supplemental Figure 6). Taken together, these data demonstrate that the S970 residue of TMEM16A is required for its association with Radixin, and that this residue is required for the effects on cell morphology and epithelial characteristics associated with increased TMEM16A expression, but does not inhibit its ability to promote cell proliferation.

Expression of TMEM16A in SCCHN Patients is Mediated via Promoter Methylation and Correlates with Epithelial Biomarkers

Since TMEM16A expression is reduced in tissues derived from metastatic nodes compared to primary tumor tissue (Figure 1), we sought to elucidate the mechanism of TMEM16A downregulation *in vivo*. We hypothesized that *TMEM16A* is transcriptionally repressed via promoter methylation during metastatic progression. Promoter methylation occurs at regions within the genome where there are high concentrations of CpG dyads (cytosines and guanines linked by a phosphodiester bonds) termed CpG islands. For *TMEM16A*, we identified a large CpG island spanning a portion of the promoter region from nucleotide (nt) −100 to +750 region relative to the transcription starting site (TSS) of *TMEM16A*. We designed primers and a probe against the bisulfite modified version of the *TMEM16A* CpG island DNA to analyze the region from nt +342 to +442 to quantitatively assess methylation (Figure 6A). To determine if the *TMEM16A* promoter region was able to undergo changes in its methylation status, 5-aza-2’-deoxycytidine (5-Aza dC) and Trichostatin A (TSA) treatments were used to un-methylate the DNA, and the percentage of 5-Aza dC induced demethylation was confirmed by comparing to its normal counterparts (Figure 6B). Expression of TMEM16A mRNA was significantly ($P<0.01$) upregulated after promoter demethylation (Figure 6C). These results demonstrate that promoter methylation can modulate the expression of TMEM16A in cancer cells.

To test our hypothesis that promoter hypermethylation modulates TMEM16A expression in metastatic nodal tissue, we obtained 5 paired primary tumor and nodal metastatic tissue samples from SCCHN patients. For each paired sample we quantified the amount of *TMEM16A* promoter methylation and subsequent mRNA expression. Methylation of the

TMEM16A promoter region was increased in the metastatic lymph node tissue (LN) (n=5; Figure 6D). Additionally, all samples demonstrated a concordant decrease in TMEM16A mRNA in the metastatic tissue (Figure 6E). Furthermore, we wanted to confirm that in these paired samples the tumor protein expression profiles were undergoing an EMT transition in the metastatic nodal tissue. Snail mRNA was increased in four of five metastatic lymph nodes when compared to paired primary tumor (Figure 6F). This change correlated with a decrease in the E-cadherin mRNA (Figure 6G), and an increase in the Vimentin mRNA validating our *in vitro* data in patient samples (Figure 6H).

Our results, taken together, provide substantial evidence that DNA methylation of TMEM16A's promoter region is directly regulating TMEM16A expression to drive changes in cell motility, migration, and morphology to promote the progression from primary tumor to metastatic nodal formation. This pleiotropic expression of TMEM16A between the primary and nodal tissue correlates with a transition from an epithelial to a mesenchymal phenotype to promote migratory and invasive capabilities of tumor cells. Finally, this process of transition is dependent upon the S970 residue in the cytoplasmic tail of TMEM16A, which is required for binding to Radixin. A model depicting the conclusions from our data shows the general mechanism by which TMEM16A promotes or inhibits tumor cell motility (Figure 6I). We have proposed a model where increased TMEM16A expression promotes tumor cell growth and an epithelial morphology, while decreased expression allows for the formation of nodal metastasis from an epithelial to mesenchymal transition (Supplemental Figure 7).

Discussion

Tumor growth and metastatic development require coordinated regulation of many cellular pathways. Often, these pathways exist in a balance, whereby tumor cells are shifted between growth and metastasis by precise molecular alterations (2). Here, we show that the promoter for *TMEM16A* is hypermethylated in metastatic tissues, and that this change in methylation is correlated with a decrease in TMEM16A mRNA and protein expression. This decrease in TMEM16A expression drives the cell towards a mesenchymal cell morphology providing enhanced migratory and metastatic capabilities (17). Additionally, reduction in TMEM16A led to the formation of smaller tumors in xenograft models, while increasing metastatic development (Figure 2). Considering this, we infer that SCCHN tumors expressing high levels of TMEM16A during their initial formation have a proliferative advantage, and during the course of metastatic progression TMEM16A is epigenetically downregulated.

Our proposed model expands on the recently suggested "Grow or Go" hypothesis for tumors that activate the Ras-ERK pathway (2). In this transformative model, during periods of growth, the Ras-Erk pathway becomes upregulated to promote proliferation and cell survival, as we have previously observed with increased TMEM16A expression (6). During the transition to the "Go" state, the Ras-Erk pathway can be downregulated to slow cell division while allowing migration and invasion to proceed. Our results serve as key evidence in support of this "Grow" or "Go" hypothesis, and highlight the importance of considering tumor growth and metastasis as independent phenomenon during the design of clinical strategies for advanced stage disease.

We posit that for a tumor cell to successfully metastasize, the cell must switch from the "Grow" morphology to its "Go" morphology. This transition requires highly coordinated regulation of gene expression, causing the cell to alter its cytoskeletal arrangements leading to mesenchymal characteristics, increased motility, and subsequent metastasis. Inferred from our data, altering *TMEM16A* promoter methylation epigenetically is likely sufficient for a tumor cell to dynamically regulate its morphology and growth characteristics during tumor progression.

Additionally, the acquisition of a mesenchymal phenotype, which we observed to be induced upon stable TMEM16A knockdown, is known to facilitate motility and dissemination of tumor cells, and to be associated with alterations in gene methylation status (17). Specifically, in breast cancer, increased hypermethylation leads to loss of E-cadherin expression in the primary tumor resulting in disruption of cell-cell adhesion, and promotion of motility and invasion. Through increased hypermethylation, the tumor cell can decrease TMEM16A expression and concomitantly drive a decrease E-cadherin expression and an increase in Vimentin expression to promote EMT and metastasis. Interestingly, in distant metastatic foci outside of the lymphatic system, a reverse process has been observed where the tumor cells undergo a re-differentiation process of mesenchymal to epithelial transition to allow for the resurgence of tumor growth within the new environment (22). This process again utilizes promoter demethylation to endogenously induce E-cadherin expression resurgence, and can be influenced by the tumor microenvironment (22,23). Taken together, our data evoke an intriguing possibility whereby an environmental sensor present within the cell, possibly TMEM16A, can induce epigenetic changes through alterations in critical gene promoter activity. These changes can subsequently lead to altered differentiation during the complex transition processes of metastasis. Recent data (Simon et al.) suggests that the anti-proliferative effects of TMEM16A knockdown are more pronounced *in vivo*, suggesting that TMEM16A may serve to transduce signaling events between the tumor cell and the microenvironment (24).

We believe TMEM16A protein expression plays a dynamic role in tumor formation and progression. As a multi-transmembrane domain Ca^{2+}-activated Cl- channel, it is uniquely positioned to serve as a tool for sensing the extracellular milieu and regulating: cell proliferation through the Ras–Raf Erk signaling pathway, morphology by promoting E-cadherin expression and modulating the actin cytoskeleton via interactions with S970 and Radixin, and cell size by increasing overall volume and area. Almaca et al. previously reported the S970 residue of TMEM16A to be important for cell swelling induced by chloride fluxes (25). Overexpression of wild-type TMEM16A, but not the TMEM16A S970A mutant led to an increase in overall cell size (Figure 5). In light of the recent report suggesting that TMEM16A can associate with the Ezrin-Radixin-Moesin (ERM) proteins to facilitate interactions between the cell membrane and the actin cytoskeleton, we hypothesized that the S970 mediated the TMEM16A-ERM interaction (21). In our proteomics evaluation of cytoskeletal and motility associated proteins we found Radixin to increase in expression with TMEM16A overexpression and decrease with shRNA knockdown. We further demonstrated that the S970 residue of TMEM16A is required for TMEM16A's association with Radixin, and that this residue is required for the effects on

cell morphology and epithelial characteristics associated with increased TMEM16A expression, independent on its ability to increase cell proliferation. These findings provide additional support for our hypothesis that TMEM16A is well positioned to influence cytoskeletal dynamics, changes in the cell shape, and modulate tumor cell motility, independently of its effects on tumor cell proliferation.

These results could seem contradictory when considering previous reports that demonstrate TMEM16A knockdown causes in fact a decrease in motility(26). We believe, however, that differences between our results and previous reports may arise from differences in experimental techniques; specifically, transient knockdown with siRNA against TMEM16A used during wound-healing assays *in vitro*, and/or by the potential for cell line variations between the studies and the lack of *in vivo* data (12,27). By employing a transient knockdown of TMEM16A these authors may not have efficiently disseminated TMEM16A's affects on growth and motility. We have previously reported that reduction in TMEM16A results in a decrease in proliferation (6) exemplifying the importance to conduct motility experiments in stably expressing cell lines to avoid potential cytotoxic effects of TMEM16A siRNA (Figure 2). In our experimental design, we have considered these potential pitfalls and conducted all experiments in stably overexpressing or knockdown cells lines. More importantly, we established our key conclusions in multiple *in vitro* and *in vivo* settings, and obtained primary and metastatic tissue samples from SCCHN patients directly confirming our experimental findings (Figures 1 and 6).

It should be noted that some authors have reported that early metastatic lesions demonstrate characteristics of MET, which is in distinction to the EMT phenotype observed in our experiments (13,14). Chao et al reported that in distant metastases E-cadherin is frequently up-regulated (suggesting MET); however, lymph node metastases do not demonstrate this phenotype (23). These data suggest that lymph node metastases (a predictor of distant metastases) can be considered to represent an in-transit state of tumor progression where tumor cells are transiently immobilized and held in a mesenchymal morphology. Our data are in agreement with this model, though we did not specifically evaluate the expression of TMEM16A in distant metastases.

The physiologic role(s) of TMEM16A are in the process of being defined, and have been shown to modulate chloride channel conductance in tumor cells, influence cellular signaling, promote tumor proliferation, and now modulate tumor morphology and metastasis through the epithelial to mesenchymal transition. In this study, we have implicated TMEM16A as a pleiotropic affecter of cell motility and morphology, who's expression can regulate a tumor cells ability to transition between growth and metastasis through the "Grow" or "Go" model. Moreover, TMEM16A's influence on tumor proliferation and metastasis appears to be opposing, and likely involves regulation through changes in phosphorylation and direct protein-protein interactions (for example, TMEM16A S970 and Radixin). In demonstrating the ability of a protein such as TMEM16A to act as a fulcrum between the homeostatic balance of tumor growth and metastasis, we implicate a specific molecular target that may be exploited in SCCHN. It has not escaped our attention that the proposed model suggests the possibility of TMEM16A inhibition leading to enhanced tumor metastases, while suppressing growth of the primary tumor. However, we believe that pharmacologic

inhibition of TMEM16A is not equivalent to gene knock-down. Given the lack of specific agents to target TMEM16A, at this time, we are unable to directly compare the effects of small molecule inhibition in contrast to gene knock-down. Further work will be need to determine if the effects of TMEM16A expression on cell motility are dependent on chloride flux through the channel, or are solely mediated by protein-protein interactions at the cell membrane.

Supplementary Material

Refer to Web version on PubMed Central for supplementary material.

Acknowledgments

This work was supported in part by the Head and Neck Cancer SPORE grant (P50-CA097190, JRG), through a Career Development Award and a Pilot Project grant from the Department of Veterans Affairs BSLR&D (UD), the PNC foundation and start-up funds from the Department of Otolaryngology University of Pittsburgh School of Medicine (UD). We acknowledge the use of the lentiviral core facilities supported by UPCI CCSG P30CA047904.

References

1. Layland MK, Sessions DG, Lenox J. The influence of lymph node metastasis in the treatment of squamous cell carcinoma of the oral cavity, oropharynx, larynx, and hypopharynx: N0 versus N+ Laryngoscope. 2005; 115:629–639. [PubMed: 15805872]
2. Gil-Henn H, Patsialou A, Wang Y, Warren MS, Condeelis JS, Koleske AJ. Arg/Abl2 promotes invasion and attenuates proliferation of breast cancer in vivo. Oncogene. 2013; 32:2622–2630. [PubMed: 22777352]
3. Caputo A, Caci E, Ferrera L, Pedemonte N, Barsanti C, Sondo E, et al. TMEM16A, a membrane protein associated with calcium-dependent chloride channel activity. Science. 2008; 322:590–594. [PubMed: 18772398]
4. Huang XX, Gollin SMS, Raja SS, Godfrey TET. High-resolution mapping of the 11q13 amplicon and identification of a gene, TAOS1, that is amplified and overexpressed in oral cancer cells. Proc Natl Acad Sci USA. 2002; 99:11369–11374. [PubMed: 12172009]
5. Britschgi A, Bill A, Brinkhaus H, Rothwell C, Clay I, Duss S, et al. Calcium-activated chloride channel ANO1 promotes breast cancer progression by activating EGFR and CAMK signaling. Proc Natl Acad Sci USA. 2013; 110:E1026–E1034. [PubMed: 23431153]
6. Duvvuri U, Shiwarski DJ, Xiao D, Bertrand C, Huang X, Edinger RS, et al. TMEM16A Induces MAPK and Contributes Directly to Tumorigenesis and Cancer Progression. Cancer Res. 2012; 72:3270–3281. [PubMed: 22564524]
7. Koppikar P, Lui VWY, Man D, Xi S, Chai RL, Nelson E, et al. Constitutive Activation of Signal Transducer and Activator of Transcription 5 Contributes to Tumor Growth, Epithelial-Mesenchymal Transition, and Resistance to Epidermal Growth Factor Receptor Targeting. Clin Cancer Res. 2008; 14:7682–7690. [PubMed: 19047094]
8. Shao C, Sun W, Tan M, Glazer CA, Bhan S, Zhong X, et al. Integrated, Genome-Wide Screening for Hypomethylated Oncogenes in Salivary Gland Adenoid Cystic Carcinoma. Clin Cancer Res. 2011; 17:4320–4330. [PubMed: 21551254]
9. Issaq HJ, Veenstra TD, Conrads TP. The SELDI-TOF MS approach to proteomics: protein profiling and biomarker identification. … and biophysical research …. 2002
10. Hood BL, Sun M, Dhir R, Conrads TP. Differential proteomic analysis of renal cell carcinoma tissue interstitial fluid. 2011
11. Rosivatz, E.; Becker, I.; Specht, K.; Fricke, E.; Luber, B. Differential expression of the epithelial-mesenchymal transition regulators snail, SIP1, and twist in gastric cancer. The American journal of [Internet]. 2002. Available from: http://www.sciencedirect.com/science/article/pii/S0002944010644641

12. Ayoub C, Wasylyk C, Li Y, Thomas E, Marisa L, Robé A, et al. ANO1 amplification and expression in HNSCC with a high propensity for future distant metastasis and its functions in HNSCC cell lines. Br J Cancer. 2010; 103:715–726. [PubMed: 20664600]
13. Wells A, Yates C, Shepard CR. E-cadherin as an indicator of mesenchymal to epithelial reverting transitions during the metastatic seeding of disseminated carcinomas. Clin Exp Metastasis. 2008; 25:621–628. [PubMed: 18600305]
14. Gunasinghe NPAD, Wells A, Thompson EW, Hugo HJ. Mesenchymal-epithelial transition (MET) as a mechanism for metastatic colonisation in breast cancer. CORD Conference Proceedings. 2012; 31:469–478.
15. Mendez MG, Kojima S-I, Goldman RD. Vimentin induces changes in cell shape, motility, and adhesion during the epithelial to mesenchymal transition. FASEB J. 2010; 24:1838–1851. [PubMed: 20097873]
16. Kalluri R. EMT: When epithelial cells decide to become mesenchymal-like cells. J Clin Invest. 2009; 119:1417–1419. [PubMed: 19487817]
17. Kalluri R, Weinberg RA. The basics of epithelial-mesenchymal transition. J Clin Invest. 2009; 119:1420–1428. [PubMed: 19487818]
18. Onder TT, Gupta PB, Mani SA, Yang J, Lander ES, Weinberg RA. Loss of E-cadherin promotes metastasis via multiple downstream transcriptional pathways. Cancer Res. 2008; 68:3645–3654. [PubMed: 18483246]
19. Keshamouni VG, Michailidis G, Grasso CS, Anthwal S, Strahler JR, Walker A, et al. Differential protein expression profiling by iTRAO-2DLC-MS/MS of lung cancer cells undergoing epithelial-mesenchymal transition reveals a migratory/invasive phenotype. J Proteome Res. 2006; 5:1143–1154. [PubMed: 16674103]
20. Zheng L, Foley K, Huang L, Leubner A, Mo G, Olino K, et al. Tyrosine 23 Phosphorylation-Dependent Cell-Surface Localization of Annexin A2 Is Required for Invasion and Metastases of Pancreatic Cancer. PLoS ONE. 2011; 2016:-e19390. [PubMed: 21572519]
21. Perez-Cornejo P, Gokhale A, Duran C, Cui Y, Xiao Q, Hartzell HC, et al. Anoctamin 1 (Tmem16A) Ca2+-activated chloride channel stoichiometrically interacts with an ezrin-radixin-moesin network. Proc Natl Acad Sci USA. 2012
22. Chao YL, Shepard CR, Wells A. Breast carcinoma cells re-express E-cadherin during mesenchymal to epithelial reverting transition. Mol Cancer. 2010; 9:179. [PubMed: 20609236]
23. Chao YY, Wu QQ, Acquafondata MM, Dhir RR, Wells AA. Partial mesenchymal to epithelial reverting transition in breast and prostate cancer metastases. Cancer Microenviron. 2012; 5:19–28. [PubMed: 21892699]
24. Simon S, Grabellus F, Ferrera L, Galietta L, Schwindenhammer B, Muhlenberg T, et al. DOG1 regulates growth and IGFBP5 in gastrointestinal stromal tumors. Cancer Res. American Association for Cancer Research. 2013; 73:3661–3670.
25. Almaca J, Tian Y, Aldehni F, Ousingsawat J, Kongsuphol P, Rock JR, et al. TMEM16 proteins produce volume-regulated chloride currents that are reduced in mice lacking TMEM16A. J Biol Chem. 2009; 284:28571–28578. [PubMed: 19654323]
26. Poulsen KA, Hoffmann EK, Schwab A. The role of TMEM16A (ANO1) and TMEM16F (ANO6) in cell migration. … -European Journal of …. 2013
27. Liu WW, Lu MM, Liu BB, Huang YY, Wang KK. Inhibition of Ca(2+)-activated Cl(–) channel ANO1/TMEM16A expression suppresses tumor growth and invasiveness in human prostate carcinoma. Cancer Lett. 2012; 326:41–51. [PubMed: 22820160]

Translational Relevance

We have previously shown that TMEM16A /ANO1 is overexpressed in squamous cell carcinoma of the head and neck. The role of TMEM16A in metastatic progression remains unclear. Our data demonstrate that expression of the oncogenic protein TMEM16A can differentially regulate tumor cell growth and metastasis. Epigenetic modification of the TMEM16A promoter facilitates the transition between cell proliferation and motility through altered TMEM16A protein expression. Mechanistically, this occurs via regulating epithelial/mesenchymal morphology. By dissociating tumor proliferation and motility, our data highlight the importance for examining metastatic characteristics independent of oncogenesis. Further, we implicate TMEM16A as a contributor to metastatic progression and highlight the role of ion channels in tumor progression.

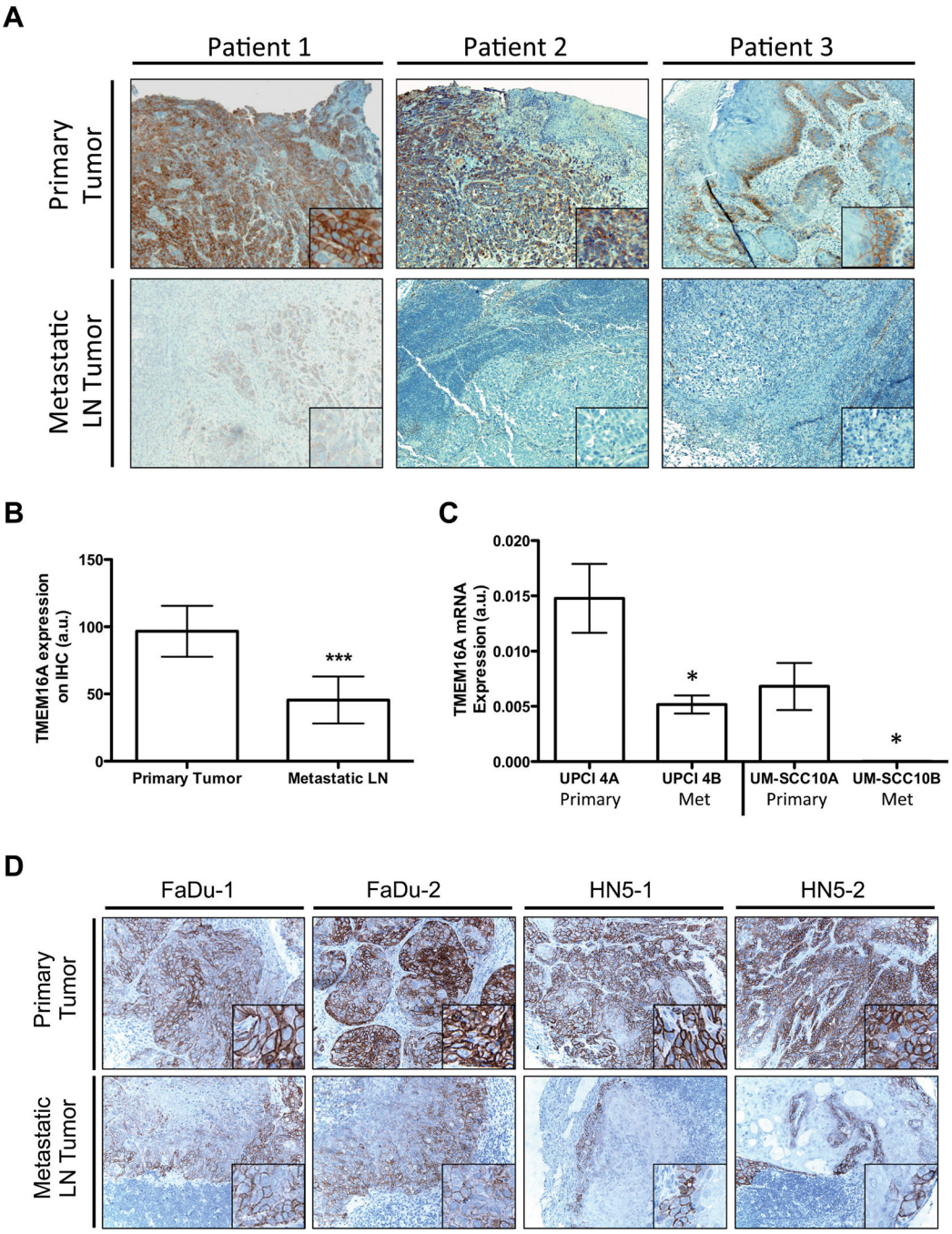

Figure 1. Expression of TMEM16A is decreased in SCCHN nodal metastatic tissue

A. Primary and metastatic tumor tissue from SCCHN patients were obtained to determine their relative expression levels of TMEM16A via immunohistochemistry. For all paired primary and metastatic samples evaluated, expression of TMEM16A (brown) appeared to decrease in the metastatic lymph node (LN) tissue compared to its paired primary tumor tissue. **B**. Quantification of the TMEM16A staining intensity demonstrated at ~50% reduction in TMEM16A expression for the metastatic tissue (mean ± STDEV, ***P<0.001, n=24). **C**. Additionally, paired cell lines derived from SCCHN primary and metastatic tumor

tissue exhibited a reduction in TMEM16A mRNA expression in the metastatically derived cell line compared to the primary tumor cell line (mean ± SEM, **P*<0.05, n=3). **D**. To suggest the possibility that TMEM16A expression was undergoing reduction upon metastatic formation, two SCCHN cell lines, FaDu and HN5, were injected into a floor of mouth mouse model. The primary tumor and metastatic lymph nodes were harvested and stained for TMEM16A expression. A pleiotropic reduction in TMEM16A expression (brown) was observed between the primary and metastatic tumors for each cell line.

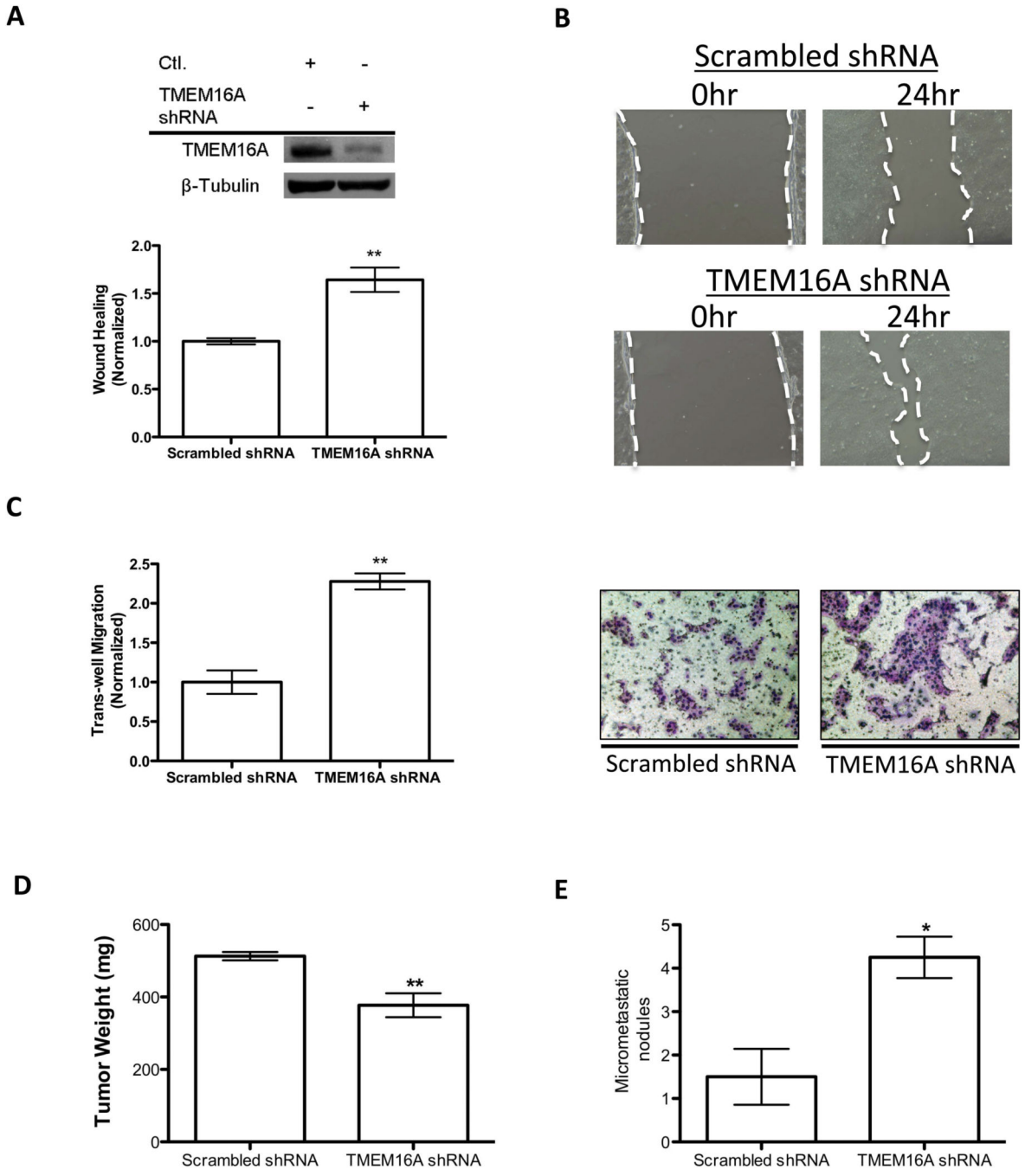

Figure 2. Knockdown of TMEM16A in SCCHN decreases motility and increases propensity for nodal metastasis

A. Immunoblotting was performed to confirm the effective knockdown of TMEM16A for these stably expressing cell lines. Wound-healing assays demonstrated an increase in motility for TMEM16A shRNA expressing SCC1 cells compared to the Scrambled shRNA control. Quantification for the change in wound healing via a difference in total area of migration resulted in a ∼65% increase for TMEM16A shRNA SCC1 cells (mean ± SEM, $^{**}P<0.01$, n=3)). **B**. Example images are shown of the differences observed in these assays.

The white dashed line outlines the area measured for each image. **C**. To further evaluate the migratory ability of cells with reduced TMEM16A expression, trans-well migration assays were performed. A significant increase in trans-well migration upon knockdown of TMEM16A was observed (mean ± SEM, ***P*<0.01, n=3). Representative fields for the trans-well migration assays used in the quantification are depicted (Right). **D**. Lastly, TMEM16A shRNA and Scrambled control SCC1 cells were implanted into a floor of mouth mouse model to evaluate to their ability to form lymph node metastatic nodules. The end primary tumor weights were measured to demonstrate the previously reported reduced growth characteristics of TMEM16A shRNA cells (mean ± SEM, ***P*<0.01, n=8). **E**. Upon termination of the experiment, mice implanted with TMEM16A shRNA expressing cells had approximately four times the amount of measurable metastatic nodules relative to the Scrambled shRNA control cells implanted mice (mean ± SEM, **P*<0.05, n=8).

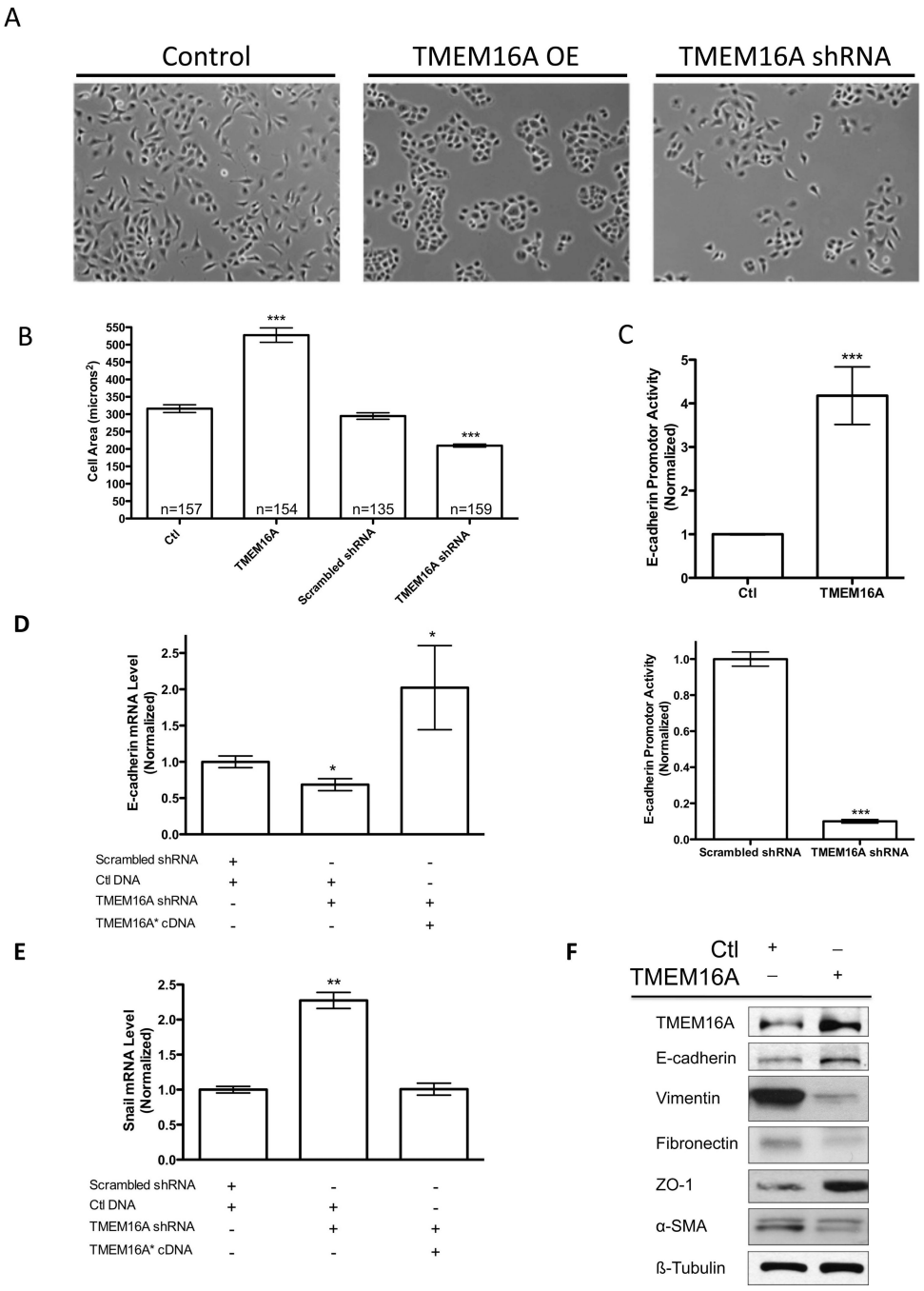

Figure 3. TMEM16A expression influences cell morphology and promotes an epithelial protein profile

A. Bright field images of T24 cancer cells show a transition from a mesenchymal morphology in control (Ctl) or TMEM16A shRNA cells to an epithelial morphology upon TMEM16A overexpression (OE). **B**. TMEM16A overexpression increased the overall cell area, while TMEM16A shRNA decreased cell area (mean ± STDEV, n= # of cells, *** *P*<0.001). **C**. Overexpression of TMEM16A was found to directly increase the E-cadherin promoter activity (Above), while TMEM16A shRNA decreased the E-cadherin promoter

activity (Bottom) (mean ± SEM, n=3, *** $P<0.001$). **D, E**. The E-cadherin promoter activity assays were supported by the ability of shRNA resistant TMEM16A* cDNA to rescue the E-cadherin mRNA expression and inversely modulate the transcriptional repressor of E-cadherin, Snail (mean ± STDEV, n=3, *$P<0.05$, **$P<0.01$). **F**. Epithelial and mesenchymal markers were evaluated in the presence and absence of TMEM16A overexpression. Increased expression of TMEM16A caused increases in epithelial markers E-cadherin and ZO-1, and resulted in decreased protein expression for mesenchymal markers Vimentin, Fibronectin, and alpha-Smooth Muscle Actin (SMA).

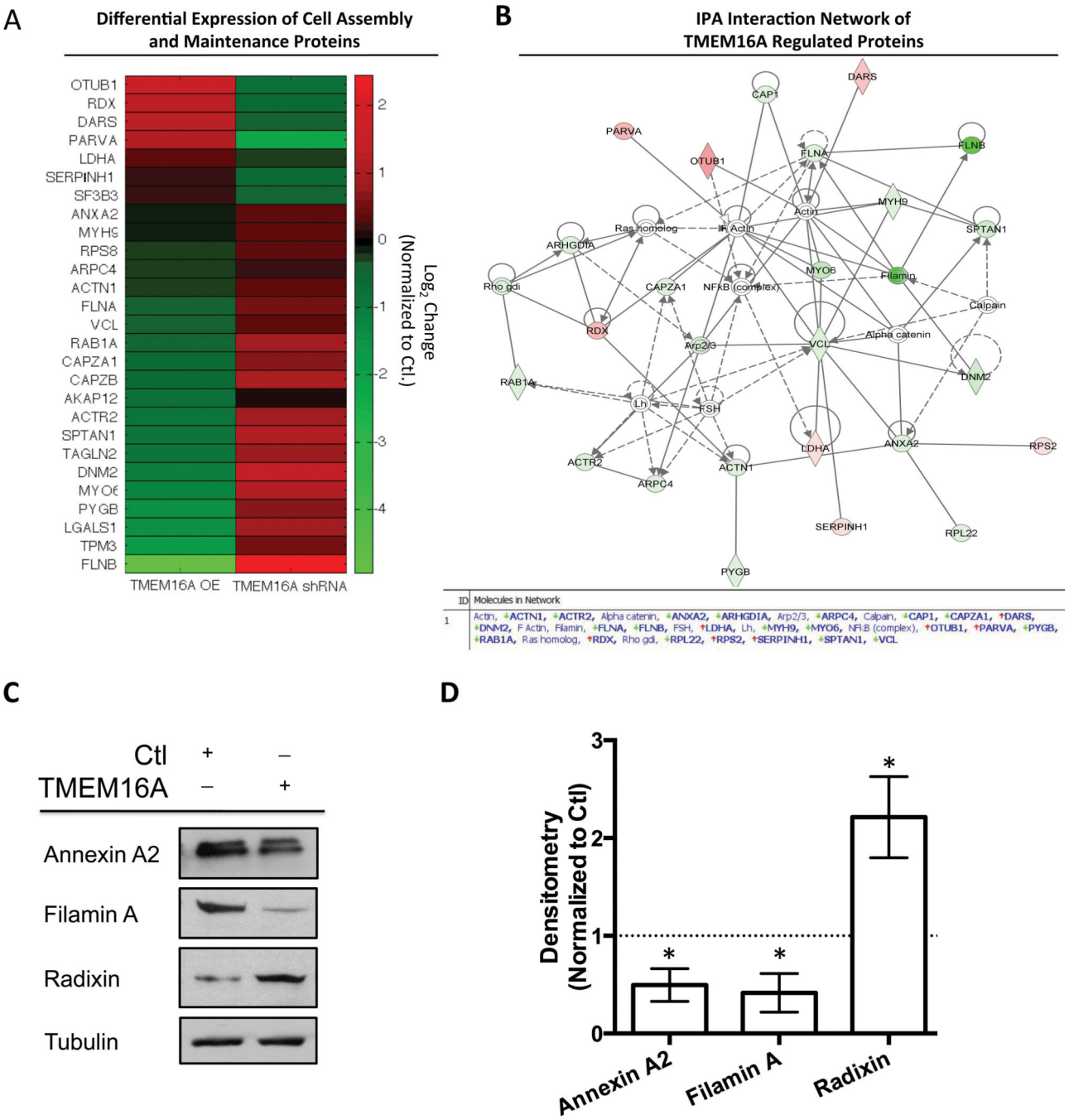

Figure 4. Broad spectrum mass spectroscopy evaluation of TMEM16A overexpression and shRNA knockdown identifies TMEM16A's regulation of motility associated proteins

A. A heatmap depicting the proteins identified as having increased expression (Red) or decreased expression (Green) is shown for the average of two independent mass spectroscopy experiments for T24 TMEM16A OE and TMEM16A shRNA cells normalized to control samples. The scale bar indicates the color associated with the Log_2 ratio change for either TMEM16A OE or shRNA compared to control cells, and the gene ID associated with each protein is labeled on the y-axis. **B**. An Ingenuity Pathway Analysis (IPA) of the

data for TMEM16A OE cells identified a cell signaling network associated with cell adhesion and motility. The red color represents an increase in protein expression, and the green color represents a decrease in the relative protein expression. **C**. Immunoblotting of Annexin A2, Filamin A, and Radixin were used to validate the results obtained from the proteomics screen. **D**. Individual immunoblotting experiments were quantified via densitometry and plotted normalized to the control cell line (dashed line) (mean ± SEM, n=3, all $P<0.05$ vs. Ctl).

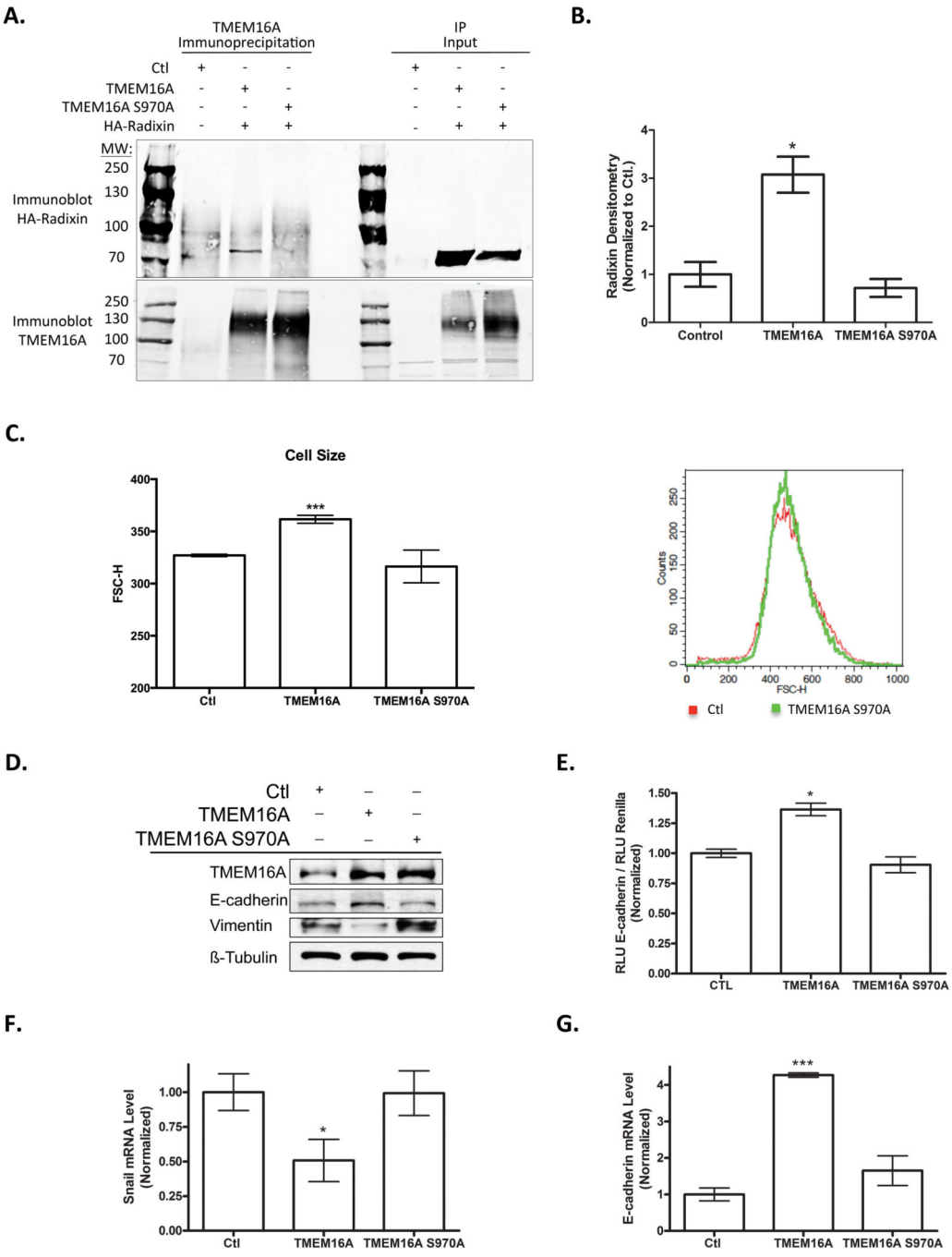

Figure 5. TMEM16A S970 Interacts Directly with Radixin and is Required for TMEM16A's Effects on Cell Morphology and EMT

A. Immunoprecipitation of TMEM16A from HEK 293 total cell lysate followed by immunoblotting of Radixin demonstrates an interaction between TMEM16A and Radixin (80kDa band) that is prevented by mutation of the S970 amino acid to alanine. **B**. Quantification of the immunoprecipitation reveals a 3-fold increase in the association between TMEM16A and Radixin that is absent with expression of TMEM16A S970A (mean ± SEM, n=3, $P<0.05$). **C**. Overexpression of TMEM16A S970A does not increase the

overall cell size as assessed by FSC-H scatter. An example of the traces obtain during flow analysis is shown. **D**. Immunoblotting reveals no change in the epithelial and mesenchymal markers E-cadherin and Vimentin upon overexpression of TMEM16A S970A. **E**. Overexpression of TMEM16A S970A does not induce the E-cadherin promoter activity (mean ± SEM, n=3, all $P<0.05$). **F**. Overexpression of TMEM16A S970A does not decrease the expression of the Snail, the transcriptional repressor of E-cadherin (mean ± SEM, n=3, all $P<0.05$). **G**. Overexpression of TMEM16A S970A does not increase the expression of the epithelial marker E-cadherin (mean ± SEM, n=3, all $P<0.001$).

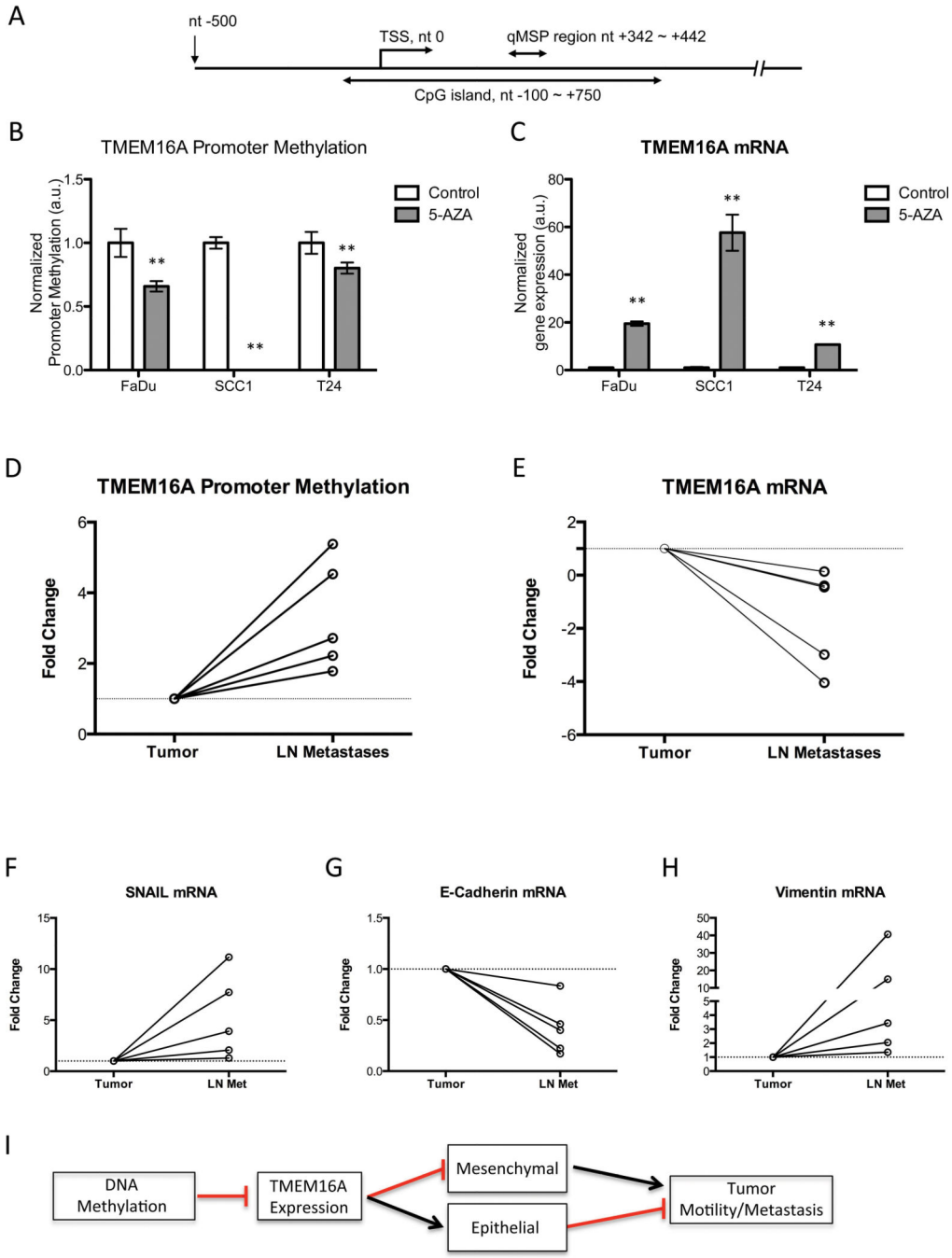

Figure 6. Expression of TMEM16A between the primary tumor to LN metastatic nodal tissue is modulated through promoter methylation

A. The *TMEM16A* genomic DNA sequence plus the 500 bp upstream region were used to determine the location of the *TMEM16A* CpG island. The transcription start site (TSS) is at position nucleotide (nt) 0, and the CpG island from nt −100 to +750. qMSP primers and probe were designed against the bisulfite-modified version of ANO1 genomic DNA, and the analyzed region covers from nt +342 to +442. **B, C**. Reduction in promoter methylation with 5-Aza dC/TSA decreased the TMEM16A promoter methylation in tumor cell lines, and

subsequently increased the TMEM16A mRNA expression (mean ± SEM, n=3, $^{**}P<0.01$). Paired primary and nodal metastatic tissue (LN Met) was obtained from SCCHN patients to assess TMEM16A promoter methylation status and mRNA expression. **D**. Hypermethylation of the TMEM16A promoter was observed in nodal metastatic tissue for each of the pairs examined. **E**. Additionally, there was a subsequent decrease in the TMEM16A mRNA expression normalized to the expression in the paired tumor sample. The two samples had an identical decrease, which is represented by the bold line. **F, G, H**. The same primary and lymph node metastatic tissue demonstrated an overall decrease in E-cadherin mRNA expression, and an increase in Vimentin and Snail mRNA expression for the primary tissue compared to the LN Met demonstrating an epithelial to mesenchymal transition. **I**. A diagram summarizing our results and TMEM16A's role in EMT and metastatic progression is shown.